

1 **Bioavailability of cobalt and iron from citric-acid-adsorbed CoFe₂O₄ nanoparticles in**
2 **the terrestrial isopod *Porcellio scaber***

3

4 Tea Romih^{a,*}, Barbara Drašler^a, Anita Jemec^a, Damjana Drobne^a, Sara Novak^a, Miha
5 Golobič^a, Darko Makovec^b, Robert Susič^c, Ksenija Kogej^c

6

7 ^aDepartment of Biology, Biotechnical Faculty, University of Ljubljana, Večna pot 111, 1000
8 Ljubljana, Slovenia

9 ^bJožef Stefan Institute, Jamova 39, 1000 Ljubljana, Slovenia

10 ^cFaculty of Chemistry and Chemical Technology, University of Ljubljana, Aškerčeva cesta 5,
11 1000 Ljubljana

12

13 ***Corresponding author: Tea Romih**

14 Department of Biology

15 Biotechnical Faculty

16 University of Ljubljana

17 Večna pot 111

18 1000 Ljubljana, Slovenia

19 Tel: +386-1-3203375

20 Fax: +386-1-2573390

21 Email: tea.romih@student.uni-lj.si

22

23

24

25 **Abstract**

26 The aim of this study was to determine whether citric acid adsorbed onto cobalt ferrite
27 (CoFe₂O₄) nanoparticles (NPs) influences the bioavailability of their constituent Co and Fe.
28 Dissolution of Co and Fe was assessed by two measures: (i) in aqueous suspension using
29 chemical analysis, prior to application onto the food of test organisms; and (ii) *in vivo*,
30 measuring the bioavailability in the model terrestrial invertebrate (*Porcellio scaber*, Isopoda,
31 Crustacea). The isopods were exposed to citric-acid-adsorbed CoFe₂O₄ NPs for 2 weeks, and
32 tissue accumulation of Co and Fe was assessed. This was compared to pristine CoFe₂O₄ NPs,
33 and CoCl₂ and Fe(III) salts as positive controls. The combined data shows that citric acid
34 enhances free metal ion concentration from CoFe₂O₄ NPs in aqueous suspension, although *in*
35 *vivo*, very similar amounts of assimilated Co were found in isopods exposed to both types of
36 NPs. Therefore, evaluation of the dissolution in suspension by chemical means is not a good
37 predictor of metal assimilation of this model organism; body assimilation of Co and Fe is
38 rather governed by the physiological capacity of *P. scaber* for the uptake of these metals.
39 Moreover, we propose that citric acid, due to its chelating properties, may hinder the uptake
40 of Co that dissolves from citric-acid-adsorbed CoFe₂O₄ NPs, if citric acid is present in
41 sufficient quantity.

42

43

44 **Keywords:** bioavailability, cobalt ferrite, nanoparticles, dissolution, citric acid, voltammetry

45

46

47 **Introduction**

48 Cobalt ferrite (CoFe_2O_4) nanoparticles (NPs) are one of the most extensively developed
49 magnetic NPs for medical purposes (Baldi et al., 2007; Mohapatra et al., 2011) and are also
50 promising candidates for many applications in commercial electronics, such as video and
51 audio tapes, high-density digital recording media, and magnetic fluids (Zi et al., 2009). Their
52 widespread use would thus indicate increasing exposure to Co in everyday life, and its
53 presence in the environment when the consumer products are discarded.

54 The toxic effects of Co are well known, and its absorption, distribution, metabolism
55 and excretion have been thoroughly reviewed by the Agency for Toxic Substances and
56 Disease Registry (ASTDR, 2004) and the World Health Organisation (WHO, 2006). The
57 newest findings on Co toxicity reported that Co^{2+} ions are the primary toxic form of Co
58 (reviewed in Simonsen et al., 2012). Therefore, Co dissolution is an important issue that needs
59 to be discussed in depth when considering the applications for Co-containing NPs.

60 It has been shown that suspensions of pristine CoFe_2O_4 NPs have a high dissolution
61 rate of Co under acidic conditions. Soler et al. (2007) reported that at pH ~ 1 , after 14 days, up
62 to 22% of the Co can be lost from CoFe_2O_4 NPs, or after 60 days, up to 30%, depending on
63 the type of acid. A high dissolution rate was also reported for Co NPs after incubation in cell
64 culture medium with pH ~ 7.4 and at 37 °C, where the dissolution was from 20% for citrate-
65 stabilised Co NPs after 72 h, 34% for bare Co NPs after 48 h, and up to 90% for cysteine-
66 stabilised Co NPs after 72 h (Horev-Azaria et al., 2011; Hahn et al., 2012). However, Papis et
67 al. (2009) and Sabbioni et al. (2012) noted that the dissolution of Co_3O_4 NPs (at 37 °C) and
68 Co NPs (temperature not reported), respectively, was negligible in deionised water, at less
69 than 1% in both cases. Moreover, an unequal dissolution rate of the constituent metals is
70 characteristic for mixed metal oxides; at pH ~ 1 , the dissolution of Co from CoFe_2O_4 NPs has
71 been reported to be ~ 2 orders of magnitude greater than that for Fe (Soler et al., 2007). These

72 data suggest that the dissolution of Co-containing NPs is a complex process and depends on
73 many factors, such as crystal structure, temperature, pH, complexing agents, and ionic
74 strength of the medium.

75 Organic ligands are widely used surface modifiers in nanoparticle preparations, to
76 stabilise them against agglomeration, to render them compatible with another phase (i.e.,
77 metal particles can be made water-soluble when appropriate groups are attached), to promote
78 their self-organisation, or to allow deliberate interactions of NPs with other molecules, NPs,
79 surfaces, or solids (Neouze & Schubert, 2008). Citric acid is one such widely used substance
80 for the coating of NPs, as it gives them a negative charge, the electrostatic forces of which
81 prevent agglomeration of the NPs in aqueous suspension (Čampelj et al., 2008; Huynh et al.,
82 2011; Tejamaya et al., 2012). It has also been reported that citric acid coating on NPs reduces
83 their toxicity, in comparison to pristine NPs with the same chemical composition (El Badawy
84 et al., 2011; Hong et al., 2011; Nguyen et al., 2013). These observations can be explained in
85 terms of strong metal ion chelating ability of citric acid, which possesses three carboxylate
86 groups and one hydroxyl group as potential ligands. Chelation alters the solubility of metals
87 and significantly influences their mobilisation and bioavailability in biological media
88 (Matzapetakis et al., 2000).

89 Although dissolution of Co-containing NPs has been shown in aqueous suspensions
90 and in cell culture media (Soler et al., 2007; Horev-Azaria et al., 2011; Hahn et al., 2012),
91 there are very few data on *in vivo* dissolution of CoFe_2O_4 NPs (i.e. inside the bodies of living
92 organisms). In our previous study (Novak et al., 2013), we showed that pristine CoFe_2O_4 NPs
93 do not enter the digestive glands of model organisms, terrestrial isopods *Porcellio scaber*
94 (Isopoda, Crustacea), and that these isopods assimilate the dissolved Co, but not the Fe. This
95 was our motivation to continue our studies on the dissolution of Co and Fe from CoFe_2O_4
96 NPs, both in suspension and *in vivo*.

97 The main goal of the present study was to establish whether citric acid adsorbed onto
98 CoFe_2O_4 NPs can influence the nanoparticle dissolution, and how this is reflected in the metal
99 assimilation of the isopods. The bioavailable share (*sensu* Riding et al., 2013) prior to feeding
100 of the isopods on citric-acid-adsorbed CoFe_2O_4 NPs was defined as the amount of dissolved
101 Co and Fe that was possible to be quantified by chemical means. We hypothesised that this
102 amount would be elevated due the presence of citric acid (Matzapetakis et al., 2000). The
103 actual bioavailability (Meyer, 2000) was estimated on the basis of the accumulated Co and Fe
104 in the digestive glands of the isopods after dietary exposure. Both of these were compared to
105 evaluate the potential additional dissolution *in vivo* and the impact of the citric acid on the
106 metal bioavailability. Co(II) and Fe(III) salts at metal concentrations the same as those in the
107 CoFe_2O_4 NPs were used as positive controls, providing information on the physiological
108 tendencies for the assimilation of Co^{2+} and Fe^{3+} .

109

110 **1. Materials and methods**

111 ***1.1 Preparation and characterisation of nanoparticle suspensions***

112 The CoFe_2O_4 NPs were synthesised by co-precipitation from aqueous solutions of Co^{2+} and
113 Fe^{3+} ions, as described by Gyergyek et al. (2012). Citric acid was adsorbed onto the surface
114 of CoFe_2O_4 NPs following the protocol of Čampelj et al. (2008) in order to provide the NPs
115 with a strong negative zeta (ζ)-potential. The pristine ('as synthesised') and citric-acid-
116 adsorbed CoFe_2O_4 NPs were characterised using transmission electron microscopy in
117 combination with energy-dispersive X-ray spectroscopy, dynamic light scattering and ζ -
118 potential measurements. Transmission electron microscopy (TEM) images were obtained
119 using a JEOL 2100 microscope (JEOL Ltd, Tokyo, Japan), operated at 200 kV. The
120 specimens for TEM were prepared by drying the aqueous suspension of NPs (pH 7) at room
121 temperature on a transparent carbon foil supported on a copper grid. Dynamic light scattering

122 (DLS) measurements of the hydrodynamic size of the particles were performed in suspensions
123 with concentration 0.1 mg of particles per mL using an Analysette 12 DynaSizer (Fritsch
124 GmbH, Idar-Oberstein, Germany). The zeta potentials of the pristine and citric-acid-adsorbed
125 CoFe₂O₄ NPs suspended in deionized water were measured with a ZetaPALS (Brookhaven
126 Instruments Corp, Holtsville, NY, USA).

127

128 ***1.2 Chemical analysis of the dissolution of CoFe₂O₄ nanoparticles***

129 Currently, the most common methods to measure dissolution are separation by dialysis or
130 centrifugal ultracentrifugation combined with metal analysis techniques, which are mainly
131 spectroscopic (e.g., atomic absorption spectrometry, inductively coupled plasma mass
132 spectroscopy), and also others, such as ion-selective electrodes (reviewed in Misra et al.,
133 2012). As effective separation of particles from the dissolved species remains a challenge,
134 other approaches are preferential, where no separation between the particles and ions is
135 mandatory (Misra et al., 2012). One of these approaches is voltammetry, which has proven to
136 be successful in a number of aquatic toxicity studies, where electrode-reactive metal species
137 have been good predictors of true bioavailability (Tubbing et al., 1994; Huang et al., 2002;
138 Huang and Wang, 2003). Electrochemical methods also enable minimal perturbation of the
139 sample, in contrast to filtration, as the possibility of ion adsorption to the filter is avoided. In
140 the present study, we tested both the spectroscopic and voltammetric approaches for their
141 accuracy, and further compared them with the true bioavailability in the test with living
142 organisms.

143 The suspensions of citric-acid-adsorbed CoFe₂O₄ and pristine CoFe₂O₄ nanoparticles
144 (NPs) in deionised water were prepared in the same way as for the *in vivo* experiments, to
145 obtain the final concentration of 2000 µg/mL Co or 5000 µg/mL Co and 3800 µg/mL Fe, or
146 9500 µg/mL Fe (the concentrations were the same as in Novak et al., 2013). Five milliliters of

147 the dispersions were ultracentrifuged at $100,000\times g$ for 30 min at $20\text{ }^{\circ}\text{C}$ (Beckman Coulter
148 L8-70M class H preparative ultracentrifuge; SW 65 Ti rotor; 5 mL thinwalled polyallomer
149 tubes). Also, the solutions of $\text{CoCl}_2\cdot 6\text{H}_2\text{O}$ and $\text{C}_6\text{H}_8\text{O}_7\cdot x\text{Fe}^{3+}\cdot y\text{NH}_3$ in the same Co or Fe
150 concentrations were centrifuged to determine whether any ions were lost during this step; i.e.,
151 due to binding to the walls of the ultracentrifuge tubes.

152 The supernatant was separated from the pellet formed by the NPs, and divided into
153 three 1.5 mL aliquots. The first aliquot was diluted with an equal volume of 1 M HCl (*pro*
154 *analysisi*; Merck, Darmstadt, Germany), the second one with an equal volume of deionised
155 water (**Supplementary Data, Figure S1**). The first two aliquots were then analysed by flame
156 atomic absorption spectrometry (Perkin Elmer AAnalyst 100; Waltham, Massachusetts, USA)
157 to determine the differences in Co and Fe ion contents between the acidified and non-acidified
158 supernatants. To check whether particles were still present in the acidified and non-acidified
159 aliquots, the supernatants were inspected by DLS using a 3D-DLS-SLS spectrometer (LS
160 Instruments GmbH, Fribourg, Switzerland). The details of the DLS instrument operating
161 parameters and data analysis are presented in the **Supplementary Data**.

162 We presumed that if the metal content quantified by flame atomic absorption
163 spectrometry for the non-acidified aliquots was lower than that in the acidified ones, this
164 would be an additional proof that the sedimentation was incomplete, as acidification would
165 cause dissolution of the remaining NPs, and therefore enable complete atomisation in the
166 flame. On the contrary, if the metal contents quantified by flame atomic absorption
167 spectrometry for the acidified and non-acidified aliquots were comparable, then this
168 conclusion could not be drawn. Such a result would mean either that the sedimentation was
169 complete, and therefore ions were the only metal species present in the supernatants, or that
170 there was relatively complete atomisation of the unsedimented NPs in the flame.

171 The original suspensions of pristine CoFe_2O_4 NPs and citric-acid-adsorbed CoFe_2O_4
172 NPs were also analysed by flame atomic absorption spectrometry for their actual Co and Fe
173 content. Prior to the analysis, the suspensions were diluted (1:1000 and 1:2500, respectively,
174 to the final concentration of $2 \mu\text{g/mL}$ Co) with 1 M HCl, and incubated in acid for 3 days for
175 complete dissolution.

176 The third aliquot of the supernatants was analysed by square-wave cathodic adsorptive
177 stripping voltammetry (SW-CAdSV) (Mirčeski et al., 2007), to determine the best possible
178 approximation to the free Co^{2+} ion content (Pesavento et al., 2009). SW-CAdSV was applied
179 using an EG&G Princeton Applied Research Model 303A stationary mercury-drop electrode
180 assembly coupled to an Autolab PGSTAT 101 potentiostat, *via* an IME303 interface. The
181 experimental approach was adapted after Pihlar et al. (1981). The working electrode was a
182 hanging mercury-drop electrode, the auxiliary electrode was a platinum wire, and the
183 reference electrode was a Ag/AgCl/3 mol/L KCl electrode (i.e., silver/silver chloride
184 electrode, SSCE). In the electrolytic cell, $20 \mu\text{L}$ supernatant was added to a mixture of 5 mL
185 deionised water, 0.5 mL 2 M $\text{NH}_4\text{Cl}/\text{NH}_3$ buffer, and $5 \mu\text{L}$ 0.1 M dimethylglyoxime, for a
186 5.525 mL total volume. Before any measurements were taken, the solution was purged with
187 N_2 for 4 min, and at all times, the headspace of voltammetric cell was continuously flushed
188 with N_2 to avoid O_2 interference. The background Co^{2+} concentration was measured before
189 each sample by substituting the supernatant with deionised water. SW-CAdSV was performed
190 first by adsorption step of 1 minute duration at -0.7 V vs. SSCE , with the magnetic stirrer
191 switched on, and followed by a square wave scan from -0.7 V to -1.3 V vs. SSCE with 25
192 mV amplitude at 50 Hz and scan rate of 50 mV/s. The method of sequential standard
193 additions was then used, adding $20 \mu\text{L}$ $0.2 \mu\text{g/mL}$ Co^{2+} standard in each step. The Co
194 concentrations were calculated by linear regression using the ChemCal package (Ranke,
195 2013) for the R statistical software (R Core Team, 2013).

196 The dissolved Co^{2+} share was calculated as the ratio between the SW-CAdSV-
197 determined Co concentration in the NP supernatant and its total content in the original NP
198 suspensions (**Tables 1, 2**). The dissolved Fe concentrations were not measured by SW-
199 CAdSV, as no assimilation of Fe in the isopods digestive glands was detected (**Figure 3**) and
200 no further calculations could be performed.

201

202 ***1.3 Test organisms***

203 Terrestrial isopods (*P. scaber*, Latreille 1804) were collected in July, 2012, from a compost
204 heap in a non-polluted location near Ljubljana, Slovenia. The isopods were kept in a terrarium
205 filled with a layer of moistened soil and a thick layer of partly decomposed hazelnut tree
206 leaves (*Corylus avellana*), alder (*Alnus glutinosa*) and birch (*Betula pendula*) leaves, and their
207 surrounding medium was maintained constantly moist. The terrarium was kept in a controlled
208 chamber at constant temperature (20 ± 2 °C) and light (16 h light, 8 h darkness) regimes.

209

210 ***1.4 Experimental set-up***

211 Two separate experiments were carried out, one with the citric-acid-adsorbed CoFe_2O_4 NPs,
212 and the other with the Fe(III) salt. The latter served as the positive control, to determine
213 whether the Fe^{3+} ions influenced the food consumption of the isopods, and whether they are
214 assimilated into their bodies when provided in the form of salt. The citric-acid-adsorbed
215 CoFe_2O_4 NPs were initially suspended in deionised water (MilliQ, Millipore, Billerica,
216 Massachusetts, USA [pH 5.7, ρ 18.5 $\text{M}\Omega\cdot\text{cm}$]) to obtain concentrations of 2000 $\mu\text{g Co/mL}$
217 and 5000 $\mu\text{g Co/mL}$ (Novak et al., 2013). Ammonium iron(III) citrate ($\text{C}_6\text{H}_8\text{O}_7 \cdot x\text{Fe}^{3+} \cdot y\text{NH}_3$,
218 16.5%–18.5% Fe content, reagent grade) was purchased from Sigma-Aldrich (St. Louis,
219 Missouri, USA). The $\text{C}_6\text{H}_8\text{O}_7 \cdot x\text{Fe}^{3+} \cdot y\text{NH}_3$ was chosen as the source of free Fe^{3+} ions because
220 other soluble iron salts are known to be highly acidic and corrosive, such as $\text{Fe}(\text{NO}_3)_3 \cdot 9\text{H}_2\text{O}$

221 and FeCl₃ (Sigma Aldrich MSDS, 2011, 2013), as was especially relevant at the high
222 concentrations used in this study. The C₆H₈O₇·xFe³⁺·yNH₃ was dissolved in deionised water
223 at 3800 mg Fe/L and 9500 mg Fe/L, which corresponded to the Fe content in the nanoparticle
224 suspensions. In the negative control groups, the food for the isopods (leaves) was spiked with
225 deionised water.

226 The experimental setup for both experiments (with the citric-acid-adsorbed CoFe₂O₄
227 NPs and with the Fe(III) salt) was the same as in our previous study (Novak et al., 2013).
228 During the experiments, the isopods were fed with hazelnut tree leaves (*C. avellana*) on
229 which suspensions of test chemicals were applied. Hazelnut leaves were collected in an
230 uncontaminated area near the Department of Biology, Ljubljana, Slovenia, and dried at room
231 temperature. The dried leaves were cut into pieces of 100 ±10 mg. Then, 100 µL of test
232 chemicals were applied per 100 mg of leaf, to obtain the final nominal concentrations of 2000
233 µg Co and 5000 µg Co per g leaf dry mass, or 3800 µg Fe and 9500 µg Fe per g leaf dry
234 mass. The test chemicals were applied evenly onto the abaxial leaf surfaces with a paintbrush
235 (Bruynzeel Holland, size 4). The leaves were left to dry at room temperature for 24 h.

236 Adult isopods of both sexes at the intermoult stages (according to Zidar et al., 1998)
237 and of >25 mg were used. The average fresh body weight of the isopods was 46 ±14 mg
238 (mean ±SD; n = 72). Both experiments consisted of feeding the isopods on metal-spiked food
239 (citric-acid-adsorbed CoFe₂O₄ NPs; Fe(III) salt) for 14 days, followed by 1 day depuration to
240 remove the metal-spiked food from the digestive system. Each isopod was placed individually
241 into a 9 cm plastic Petri dish to which individual pieces of chemical-spiked dry leaves were
242 added. No substrate was used. All of the Petri dishes were kept in a large glass container
243 under controlled conditions, in terms of the air humidity (≥80%), temperature (21 ±1 °C) and
244 light regime (16:8 h light:dark photoperiod). The food was not replaced during the exposure
245 period, and fecal pellets were collected weekly. At the end of the experimental period, the

246 remnants of the leaves were collected, air dried, and weighed. Fecal pellets were also weighed
247 after drying in a desiccator for 24 h. The isopods were decapitated and the digestive glands
248 were isolated with tweezers. The glands were placed on separate small pieces of filter paper
249 (approximately 4 mm × 7 mm in size) and stored in plastic tubes until analysis by flame
250 atomic absorption spectrometry.

251

252 ***1.5 Flame atomic absorption spectrometry of Co and Fe content in organic material***

253 The Co and Fe contents were measured in the isopod digestive glands (hepatopancreas) and in
254 the remnants of leaves after the experiments. Prior to analysis, samples were digested in a
255 heating block with a mixture of concentrated nitric (65% HNO₃, *pro analysi*; Merck;
256 Darmstadt, Germany), and perchloric acid (70% HClO₄, *pro analysi*; Merck; Darmstadt,
257 Germany) (HNO₃:HClO₄ = 7:1, v/v). After evaporation of the acid, the residue was dissolved
258 in 0.2% HNO₃. The total Co and Fe concentrations in the digestive glands were analysed with
259 a flame atomic absorption spectrometer (Perkin Elmer AAnalyst 100; Waltham,
260 Massachusetts, USA). Within each measurement, a certified reference material (TORT-2,
261 National Research Council of Canada) was used to check the accuracy and precision of the
262 analytical procedures. Along with the samples, 20 replicates of a known amount of certified
263 reference material were also acid digested, and each sample was measured in triplicate. The
264 calculations followed the approach of Jorhem (2004) and Phillips et al. (2007). The certified
265 concentration of Co in the reference material was 0.51 ±0.09 mg/kg; our measurement was
266 0.64 ±0.14 mg/kg (mean±SD, n = 60), $Z' = 2.62$. For Fe, the certified concentration in the
267 reference material was 105 ±13 mg/kg; our measurement was 101 ±14 mg/kg (mean ±SD, n =
268 60), $Z' = -0.63$.

269

270

271 **1.6 Data analysis**

272 In both experiments, 12 isopods per test regimen were exposed to the citric-acid-adsorbed
273 CoFe_2O_4 NPs or the Fe(III) salt, although the numbers of isopods in the final analyses were
274 lower due to the mortality caused by moulting, and due to the development of marsupia in the
275 females. All of these isopods were excluded from further data processing (total lost from the
276 analysis, $n = 9$), and the numbers of the analysed animals are presented as part of the Figures.
277 The formulae for all of the calculations that were used in the present study (feeding
278 parameters of isopods, metal assimilation and the share of ions that dissolved from the
279 nanoparticles) are provided in the **Supplementary Data**, as Equations (S6) to (S9). The data
280 are presented as means, and the uncertainties are expressed as \pm standard deviations (\pm SD).
281 Statistically significant differences between the control and the exposed groups of isopods
282 were subjected to Mann-Whitney *U*-tests (*, $p < 0.05$; **, $p < 0.01$; ***, $p < 0.001$) using the
283 Statgraphics software (Statgraphics Plus for Windows 4.0, Statistical Graphics, Herndon, VA,
284 USA).

285 For the purpose of the comparisons and the discussion, the present study includes also
286 the (adapted) data from the pristine CoFe_2O_4 nanoparticles and CoCl_2 experimental systems
287 of our previous study of Novak et al. (2013), with permission from ACS Publications (Novak
288 et al., 2013. Cellular internalisation of dissolved cobalt ions from ingested CoFe_2O_4
289 nanoparticles: *in vivo* experimental evidence. *Environmental Science and Technology*, 47 (10),
290 5400–5408; Copyright, American Chemical Society, 2014). We have here reused the data and
291 adapted the Figures for the feeding rates (**Supplementary Data, Figure S3**) and the Co and
292 Fe assimilation (**Figure 3**), and we have included these data in the calculations of the metal
293 bioavailability (**Table 2**).

294

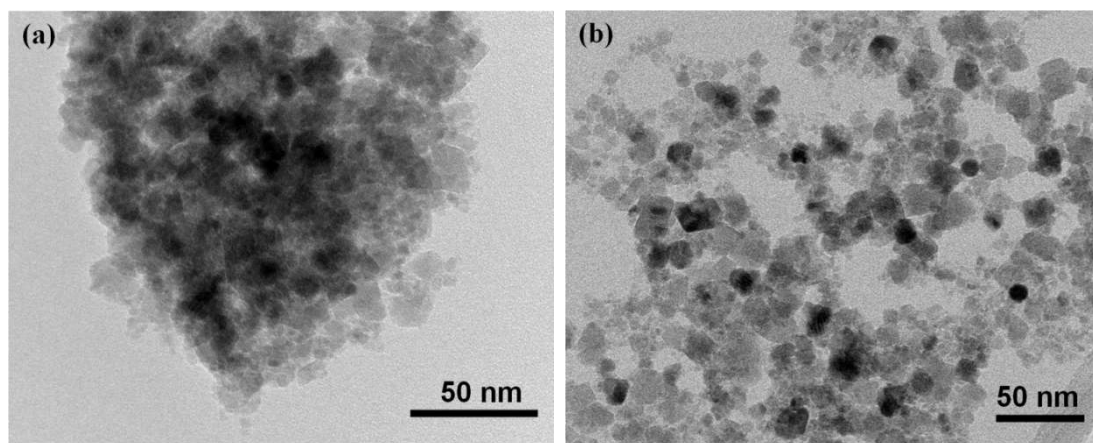
295

296 **2. Results**

297 **2.1 Characteristics of the pristine and citric-acid-adsorbed CoFe₂O₄ nanoparticles**

298 Transmission electron microscopy showed a size distribution of the pristine CoFe₂O₄
299 nanoparticles from 5 nm to >15 nm with the presence of larger agglomerates (**Figure 1a**),
300 whereas citric-acid-adsorbed CoFe₂O₄ NPs were present as individual NPs or formed smaller
301 agglomerates, <50 nm in size (**Figure 1b**). The energy-dispersive X-ray spectroscopy analysis
302 showed a composition that matched the stoichiometry of CoFe₂O₄.

303



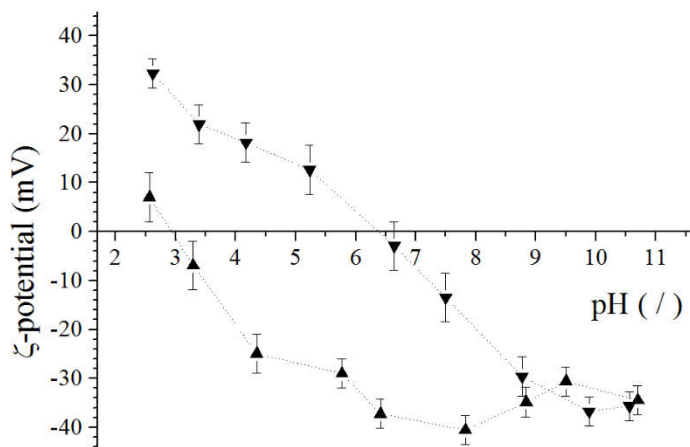
304

305 **Figure 1.** Representative transmission electron microscopy images of the pristine CoFe₂O₄ nanoparticles (**a**) and
306 the citric-acid-adsorbed CoFe₂O₄ nanoparticles (**b**).

307

308 As the pristine CoFe₂O₄ NPs in the aqueous suspension agglomerated strongly, the DLS
309 measurements were not reliable. Suspension of the citric-acid-adsorbed CoFe₂O₄ NPs in
310 deionised water formed agglomerates with around 210 nm in size, although agglomerates >1
311 μm were also present. The ζ-potentials of both the pristine CoFe₂O₄ NPs and the citric-acid-
312 adsorbed CoFe₂O₄ NPs were measured across the complete pH range. The aqueous
313 suspension of the pristine CoFe₂O₄ NPs had an isoelectric point at pH 7. The citric-acid-
314 adsorbed CoFe₂O₄ NPs had an isoelectric point at pH ~3 and a strong negative ζ-potential at

315 neutral pH (between -35 mV and -40 mV), due to the citric acid ions on their surface (**Figure**
316 **2**).
317



318
319 **Figure 2.** ζ-Potential of the pristine (▼) and citric-acid-adsorbed (▲) CoFe₂O₄ nanoparticles dispersed in
320 deionised water, as a function of the pH of the suspensions.
321

322 *2.2 Dissolution of Co and Fe in suspensions of the pristine and citric-acid-adsorbed* 323 *CoFe₂O₄ nanoparticles*

324 The total concentrations of Co and Fe in NP suspensions and salt solutions used for the
325 feeding experiments were generally in good agreement with the nominal values (less than
326 10% deviation), with the exception of the highest concentration of Co in the case of the
327 pristine CoFe₂O₄ NPs, which was higher by 30% (**Table 1**).

328 Centrifugation did not remove any Co²⁺ or Fe³⁺ from the supernatants, as shown by the
329 data for CoCl₂ and C₆H₈O₇·xFe³⁺·yNH₃ (**Supplementary Data, Table S1**). The DLS
330 measurements of the non-acidified supernatants of both the pristine and citric-acid-adsorbed
331 CoFe₂O₄ NPs showed that NP were still present (**Supplementary Data, Figure S2**). For the
332 supernatant of the pristine CoFe₂O₄ NPs, the scattering intensity at the detector was very low

333 (approximately 15-25 kHz at the maximum incident laser intensity), which indicates that the
334 unsedimented particle share was very small. For the citric-acid adsorbed CoFe_2O_4 NPs, much
335 larger share of particles remained in the supernatant as the scattering intensity was much
336 higher (>100 kHz at the maximum incident laser intensity). In the acid-diluted samples, the
337 scattering intensity at the detector was the same as that of the pure solvent (approximately 3-4
338 kHz at the maximum incident laser intensity). Moreover, in the limit of the sensitivity of the
339 DLS technique, the measurement did not indicate any large particles ($R_h \approx 100$ nm) in
340 solution. This demonstrates that the particles completely dissolved in the acid. For this reason,
341 we cannot provide any graphs of the particle size distributions.

342 However, the atomic absorption spectrometry measurements did not yield a significant
343 difference between the metal concentrations of each of the acidified and non-acidified
344 supernatant aliquots (**Supplementary Data, Table S1**), therefore we concluded that
345 unsedimented NPs were atomised in the flame and the atomic absorption spectrometry
346 technique must have overestimated the free ion content. Accordingly with the DLS data, the
347 concentrations of Co and Fe in the supernatants as measured by AAS were significantly
348 higher for the citric-acid-adsorbed CoFe_2O_4 NPs compared to the pristine CoFe_2O_4 NPs
349 (**Table 1**). The estimations of Co^{2+} content in NP supernatants obtained by SW-CAdSV were
350 lower than the ones by AAS, which confirmed that SW-CAdSV enables better quantification
351 of the dissolved Co^{2+} for both the pristine and the citric-acid-adsorbed CoFe_2O_4 NPs (**Table**
352 **1**).

353

354 Please insert Table 1 here

355

356 We made no attempt to determine the concentrations of Fe ion species in the
357 supernatants by electrochemical means, because the primary focus was on Co, which showed

358 a tendency to accumulate in the digestive glands of the isopods when they were fed with both
359 the pristine CoFe_2O_4 NPs (Novak et al. 2013) and the citric-acid-adsorbed CoFe_2O_4 NPs
360 (**Figure 3a**). In contrast, no assimilation of Fe was detected in the digestive glands (**Figure**
361 **3b**). The values determined for the flame atomic absorption spectrometry of Fe in the
362 supernatants of both the pristine and the citric-acid-adsorbed CoFe_2O_4 NPs correspond to
363 those obtained for Co (**Supplementary Data, Table S1**), and are therefore likely to denote
364 the total value of unsedimented NPs, and not ions.

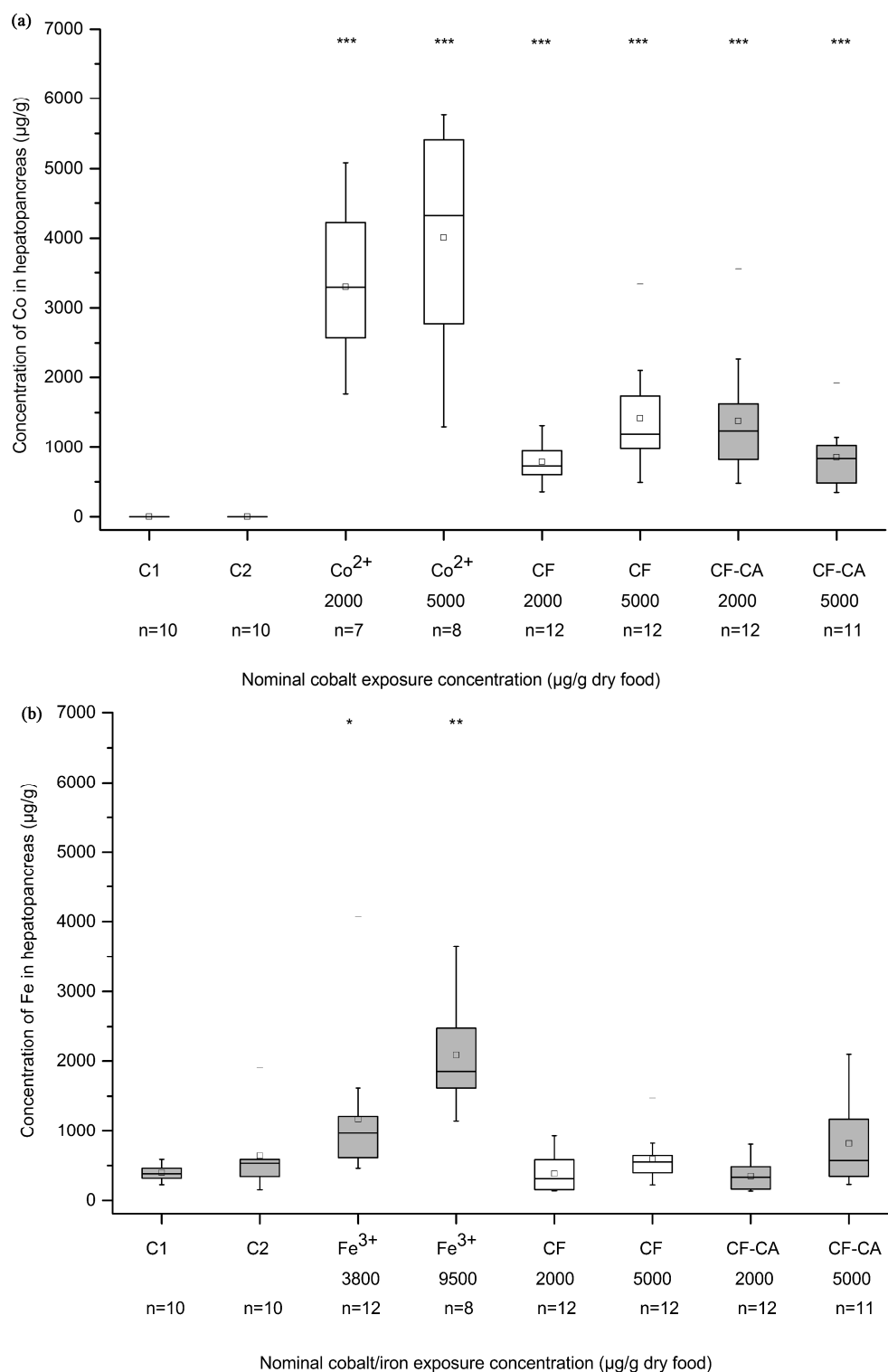
365

366 *2.3 Metal content in the digestive gland tissue*

367 After the 14-day exposure of the isopods to the citric-acid-adsorbed CoFe_2O_4 NPs, the Co
368 contents in the digestive glands of both treated groups rose significantly, in comparison to the
369 controls (**Figure 3a**). There were no significant differences ($p > 0.05$; not marked on Figure
370 3a) between the isopods exposed to the different concentrations of the citric-acid-adsorbed
371 CoFe_2O_4 NPs. For clarity, we also compared our results with the ones from Novak et al.
372 (2013). The isopods exposed to the citric-acid-adsorbed CoFe_2O_4 NPs accumulated less Co
373 than the CoCl_2 -exposed ones (Novak et al., 2013). At the lower exposure concentration (2000
374 $\mu\text{g Co/g dry leaf}$), the isopods exposed to the citric-acid-adsorbed CoFe_2O_4 NPs accumulated
375 significantly more Co ($p < 0.05$; not marked on Figure 3a) than the isopods exposed to the
376 pristine CoFe_2O_4 NPs (Novak et al., 2013), while at the higher exposure concentration (5000
377 $\mu\text{g Co/g dry leaf}$), the situation was reversed ($p < 0.05$; not marked on Figure 3a).

378 The data shown in **Figure 3b** were obtained according to the two separate
379 experiments, with the first set of isopods exposed to citric-acid-adsorbed CoFe_2O_4 NPs, and
380 the second set exposed to the Fe(III) salt. The corresponding control groups are shown as
381 Control 1 and Control 2, respectively, and there were no statistical differences between these
382 controls (**Figure 3b**). The hepatopancreatic Fe content increased significantly in comparison

383 to the controls only in the groups exposed to Fe(III) salt ($p < 0.01$), and hence not for the
384 isopods exposed to the citric-acid-adsorbed CoFe_2O_4 NPs (**Figure 3b**). Significant differences
385 in the Fe concentrations were seen between the two exposure concentrations of Fe^{3+} ($p < 0.01$;
386 not marked on Figure 3b).
387



388

389 **Figure 3.** Concentration of Co (**Fig.1a**) or Fe (**Fig.1b**) in hepatopancreas of *P. scaber* fed for 14 days on food
 390 dosed with CoCl_2 (Co^{2+}), Fe(III) salt (Fe^{3+}), pristine CoFe_2O_4 nanoparticles (CF) or citric-acid-adsorbed CoFe_2O_4
 391 nanoparticles (CF-CA). Symbols on the box plot represent minimum and maximum data values (whiskers),
 392 mean value (\square), 75th percentile (upper edge of the box), 25th percentile (lower edge of the box), median (line in
 393 the box), max and min value (\perp), and outliers (-). Statistically significant differences between exposed and

394 control isopods (C1, C2; both controls were generated in this study) are indicated by *** ($p < 0.001$). Data for
395 groups of isopods exposed to CoCl_2 and both nanoparticles were compared to Control 1, while isopods exposed
396 to the Fe(III) salt were compared to Control 2. There were no significant differences in the amounts of Fe
397 between the isopods in the control groups from the two experiments. Nominal exposure concentrations (2000 μg
398 or 5000 μg Co/g of leaf, or 3800 μg or 9500 μg Fe/g of leaf; originated from Co or Fe salts or from suspensions
399 of pristine CoFe_2O_4 or citric-acid-adsorbed CoFe_2O_4 nanoparticles) are provided on the x-axes. N, number of
400 isopods that were analysed in each group (from 15 per group exposed at the beginning of the feeding). For the
401 purposes of comparison, the unshaded box plots are reprinted (adapted) with permission from Novak et al. 2013
402 (Cellular internalisation of dissolved cobalt ions from ingested CoFe_2O_4 NPs: *in-vivo* experimental evidence.
403 *Environmental Science and Technology*, 47 (10), 5400–5408). Copyright (2014) American Chemical Society.

404

405 ***2.4 The role of in vivo dissolution of pristine and citric-acid-adsorbed CoFe_2O_4*** 406 ***nanoparticles on the assimilation of Co into the hepatopancreas***

407 As only Co showed a tendency to assimilate into the hepatopancreas when the isopods were
408 exposed to the CoFe_2O_4 NPs (**Figure 3**), we did not further analyse the bioavailability of Fe.
409 On the basis of the measured concentrations of dissolved Co^{2+} for both the pristine and the
410 citric-acid-adsorbed CoFe_2O_4 NPs in suspension and before application to the isopod food
411 (**Table 1**), and considering the amount of consumed leaves during the two experiments, we
412 calculated the hypothetical concentrations of Co in the hepatopancreas in case only the free
413 ions were assimilated and no additional dissolution occurred in the isopod digestive system
414 (**Table 2**). We compared these concentrations to those measured for Co in the hepatopancreas
415 (**Table 2**). For the pristine CoFe_2O_4 NPs (data adapted from Novak et al., 2013), the actual
416 assimilation was significantly higher than the calculated one (**Table 2**; $p < 0.001$, for both
417 exposure concentrations). However, with the citric-acid-adsorbed CoFe_2O_4 NPs, the
418 difference was present only at the lower exposure concentration (**Table 2**; $p < 0.001$ for 2000
419 μg Co/g dry food, and $p > 0.05$ for 5000 μg Co/g dry food). The formulae (**Equations (S6)-**
420 **(S9)**) used are provided in the **Supplementary Data**.

421 Please insert Table 2 here

422

423 **3. Discussion**

424 The results of this study show that citric acid enhances free Co^{2+} concentration from the citric-
425 acid-adsorbed CoFe_2O_4 NPs in comparison to the pristine CoFe_2O_4 NPs in aqueous
426 suspension. Additional dissolution of Co from both the pristine and the citric-acid-adsorbed
427 CoFe_2O_4 NPs occurred also in the isopod digestive system, independently of the presence of
428 citric acid. However, in the feeding experiments very similar amounts of assimilated Co were
429 found regardless of the citrate modification of NPs. We argue that citric acid may hinder the
430 uptake of Co by the isopods due to its chelating properties, which are favoured by the near-
431 neutral pH of their gut. Furthermore, the assimilation of the Fe dissolved from both types of
432 CoFe_2O_4 NPs was negligible due to the low physiological capacity of *P. scaber* for the uptake
433 of Fe into their digestive glands.

434 If the concentration of the dissolved metal ion species is to be accurately determined,
435 reliable separation of the dissolved fraction from remaining NPs needs to be ensured, or
436 methods that are sensitive only to ions need to be employed. As several papers have pointed
437 out, the combination of ultracentrifugation and spectroscopic methods often overestimates the
438 free ion share (David et al., 2012; Misra et al., 2012; Xu et al., 2013), therefore voltammetry
439 is a better choice for the dissolution studies (David et al., 2012; Jiang and Hsu-Kim, 2014).
440 The free ion shares obtained by the two methods correlate closely only when the
441 centrifugation is performed at very high speeds and long durations (Jiang and Hsu-Kim,
442 2014). This was also confirmed in our study, where we showed by both flame AAS and DLS
443 assessment of the supernatants of CoFe_2O_4 NPs that centrifugation at 100000 g for 30 min
444 did not suffice to sediment the NPs, neither pristine nor the citric-acid-adsorbed ones
445 (**Supplementary Data, Figure S2**). The flame AAS therefore necessarily overestimated the

446 dissolved metal share (**Table 1**), even if the samples were not acidified (**Supplementary**
447 **Data, Table 1**). We propose voltammetry as one of the method of choice for the accurate and
448 direct quantification of the dissolved metal species, especially for the metals for which the
449 commercially-available ion-selective electrodes do not exist (Pesavento et al., 2009).

450 In suspensions of citric-acid-adsorbed CoFe_2O_4 NPs, a fraction of the citric acid is not
451 adsorbed and remains in solution and in equilibrium with the adsorbed citric acid (Čampelj et
452 al., 2008). Citric acid is known to mediate chelation-induced dissolution (Matzapetakis et al.,
453 2000; Hajdú et al., 2009), which was reflected in the voltammetrically determined Co^{2+}
454 concentration in the supernatants of CoFe_2O_4 NPs. The supernatants of the pristine CoFe_2O_4
455 NPs contained some $\mu\text{g/L}$ of the dissolved Co^{2+} , while the dissolved Co^{2+} content reached
456 some tens of mg/L of the citric-acid-adsorbed CoFe_2O_4 NPs (**Table 1**). However, we cannot
457 exclude the possibility that the citrate- Co^{2+} complexes reacted indiscriminately at the
458 electrode, so the term “dissolved” in this context should encompass all the Co^{2+} that was not
459 bound to nanoparticles, regardless whether it was present in the form of chelates with the
460 citric acid or free in the solution.

461 The difference in the dissolved metal content in the NP suspensions used for the *in*
462 *vivo* experiments was not reflected in the uptake of metals by isopods, where the citric acid
463 adsorbed onto the CoFe_2O_4 NPs did not affect the assimilation of Co or Fe in the digestive
464 glands (**Figure 3, Table 2**). This indicates that the evaluation of dissolution in suspension by
465 chemical means is not a good predictor of actual metal assimilation in the digestive system of
466 isopods *P. scaber*. Instead, distinct metal dissolution and assimilation processes must have
467 taken place inside the test organisms. This finding has implications for *in silico* approaches to
468 predict metal bioavailability, where the discrepancy between the chemical estimates and *in*
469 *vivo* approaches should be taken into consideration.

470 As in our previous study (Novak et al., 2013), Co and Fe showed different tendencies
471 for assimilation into the digestive glands of the model organisms in both experiments
472 presented here (**Figure 3**). The presence of Co in the digestive glands was observed after the
473 isopod feeding on the citric-acid-adsorbed CoFe_2O_4 NPs (**Figure 3a**), although the amount of
474 Co was lower in comparison to the animals fed on the CoCl_2 at the same concentration
475 (**Figure 3a**; Novak et al., 2013), regardless of the lowered feeding rate of the CoCl_2 -exposed
476 isopods (**Supplementary Data, Figure S3**). Fe was accumulated when the isopods were
477 exposed to both concentrations of the Fe(III) salt, but not when they were fed on either the
478 pristine (**Figure 3b**; Novak et al., 2013) or the citric-acid-adsorbed CoFe_2O_4 NPs containing
479 the same concentrations of Fe (**Figure 3b**). The data from the Fe(III) salt shows that the
480 amount of free Fe^{3+} ions must be very high for even a small amount of Fe^{3+} to be assimilated
481 (**Figure 3b**). The same observation was noted already by Hopkin (1990a), who discovered
482 that the majority of Fe from the metal-polluted leaves was retained in the gut of the *P. scaber*
483 and later excreted, while some other metals, such as Cd, Cu, Pb and Zn, became assimilated
484 into the hepatopancreas in large quantities. The difference in the assimilation tendencies for
485 different metals is a consequence of the different pathways of their uptake and storage in the
486 hepatopancreatic cells of *P. scaber* (Hopkin, 1990b). While Co follows the Type B pathway,
487 which is the same as for Cu and other metals with the affinity for sulphur-bearing ligands
488 (Hopkin, 1990b; Novak et al., 2013), Fe follows a specific pathway designated Type C, and
489 binds to haemosiderin, a breakdown product of ferritin (Hopkin, 1990b).

490 As the physiological capacity of the isopods to assimilate Fe^{3+} was confirmed to be
491 extremely low *per se*, despite its bioavailability (*sensu* Riding et al., 2013), we concentrated
492 exclusively on the *in vivo* dissolution of Co^{2+} . To evaluate the role of the isopods in the
493 dissolution of the CoFe_2O_4 NPs, we compared (i) the hypothetical concentrations of Co in the

494 hepatopancreas (on the basis of the voltammetric determination), to (ii) the actual measured
495 concentrations of Co in the hepatopancreas.

496 For the pristine CoFe_2O_4 NPs (Novak et al., 2013), the measured hepatopancreas
497 concentrations of Co were 4-5 orders of magnitude higher than those calculated (**Table 2**).
498 Therefore, a large proportion of the Co^{2+} must have dissolved in the digestive system during
499 feeding. This was confirmed also by the absence of Co and Fe co-localisation in the cells, as
500 shown by the low-energy X-ray fluorescence microscopy, which indicates that only Co^{2+} , and
501 not the whole NPs, entered the cells (Novak et al., 2013). However, in the case of the citric-
502 acid-adsorbed CoFe_2O_4 NPs, the measured concentrations of Co were higher than calculated
503 at the lower exposure of 2000 $\mu\text{g Co/g}$ dry leaf mass, but the same at the higher exposure of
504 5000 $\mu\text{g Co/g}$ dry leaf mass (**Table 2**). We can therefore confirm that there was additional
505 dissolution of Co from the citric-acid-adsorbed CoFe_2O_4 NPs after consumption only for the
506 lower exposure (2000 $\mu\text{g Co/g}$ dry leaf mass). At the higher exposure (5000 $\mu\text{g Co/g}$ dry leaf
507 mass), the dissolved (voltammetrically determined) Co was the same as the bioavailable Co
508 share ($p>0.05$; **Table 2**). However, the data from CoCl_2 shows that the isopods would be able
509 to assimilate even more Co^{2+} from CoFe_2O_4 NPs if more was bioavailable; it is expected that
510 the dissolution of particulate matter is slower than that of the soluble salts, so the dissolution
511 of CoFe_2O_4 NPs in the isopod digestive system was probably limited in the given exposure
512 period.

513 A closer look at the experimental results for the higher exposure concentrations also
514 reveals that the isopods fed on the citric-acid-adsorbed CoFe_2O_4 NPs assimilated less Co
515 compared to those fed on the pristine CoFe_2O_4 NPs (**Figure 3a**; $p < 0.05$). A possible
516 explanation for this might lie in the chelation of Co^{2+} by the citric acid. Namely, suspensions
517 with higher concentrations of citric-acid-adsorbed CoFe_2O_4 NPs contain a larger amount of
518 citric acid that is not bound to particles (Čampelj et al., 2008) and that is therefore free to

519 chelate metal ions that are released from the NPs (Matzapetakis et al., 2000). The stability
520 constant of the Co^{2+} -citrate complex is 4.4 (Furia, 1972), which means that the dissociation to
521 Co^{2+} from the citric acid is not favoured in non-acidic environments (Furia, 1972), as is the
522 case in the isopod digestive tract (Zimmer & Topp, 1997; Zimmer & Brune, 2005).

523 It has been shown that a large proportion of the Co dissolves from the pristine
524 CoFe_2O_4 NPs under acidic conditions, at pH \sim 1 (Soler et al., 2007), which is comparable to
525 the conditions in the vertebrate stomach. However, measurements with a pH microelectrode
526 in the gut of *P. scaber* showed pH 5.5 to pH 6.0 in the anterior hindgut, and pH 6.0 to pH 6.5
527 in the posterior hindgut (Zimmer & Topp, 1997). In the hepatopancreas, the pH is 5.8 to 6.4 in
528 the proximal region, and 5.8 to 6.1 in the distal region (Zimmer & Brune, 2005). Therefore,
529 the dissolution of Co from the CoFe_2O_4 NPs inside the digestive tract is more likely to be of a
530 chelating/ligand-promoted type than protonation-induced. It is known that very high
531 concentrations of surfactant lipids are present in the gut fluid of isopods, to reduce the
532 potential impact of ingested tannins via their food (Zimmer, 1997). These substances, along
533 with other constituents of the isopod gut content, are likely to be the cause of enhanced
534 dissolution of CoFe_2O_4 NPs inside the digestive tract, despite it being only a slightly acidic
535 environment. Also, studies of metal solubilisation in polluted marine sediments with digestive
536 juices extracted from representatives of different marine invertebrate taxa have showed that
537 the digestive juices can significantly mobilise sediment-bound metals, even though their pH
538 was close to 7 (Lawrence et al., 1999; Mayer et al., 2001; Weston and Maruya, 2002).

539

540 **4. Conclusions**

541 We propose that the assimilation of Co dissolved from consumed CoFe_2O_4 NPs is very
542 complex and depends on several factors inside the isopod digestive system. Dissolution of
543 NPs in suspension and additional dissolution *in vivo* due to the specific digestive juice

544 composition make the most important contributions here, while citric acid plays a dual role if
545 it is present in sufficient amounts: it enhances the NP dissolution in suspension, but hinders
546 the metal assimilation *in vivo*. However, citric acid does not entirely prevent the assimilation
547 of Co into the digestive glands, which shows that citric-acid-adsorbed CoFe₂O₄ NPs are not
548 chemically inert in contact with living organisms. Finally, the metal assimilation *in vivo* is
549 critically controlled also by the propensity of the isopods for the uptake of the metal in
550 question, which is evident from the difference between Co and Fe. This shows that chemical
551 methods alone are not sufficient for the proper evaluation of the bioavailability of NPs; it is
552 crucial that they are combined with *in vivo* experiments with such model organisms which
553 enable precise quantification of the NP uptake.

554

555 **Acknowledgements**

556 This study is part of the PhD projects of Tea Romih and Barbara Drašler, both of whom are
557 working under the supervision of Professor Damjana Drobne. The investigation was
558 supported by the Ministry of Education, Science, and Sport of the Republic of Slovenia, under
559 the system of the “Innovative scheme of co-funding doctoral studies for promoting
560 cooperation with the economy and solving contemporary social challenges”, under grant
561 numbers 160-21 (B. Drašler) and 1291 (T. Romih). This study also received funding from the
562 European Community Seventh Framework Programme (FP7/2007-2013) under grant
563 agreement number 263147-NanoValid, and from the Slovenian Research Agency (ARRS)
564 under grant agreement number J1-4109. The funding sources were not involved in the study
565 design; in the collection, analysis and interpretation of data; in the writing of the manuscript;
566 or in the decision to submit the manuscript for publication.

567 The authors would like to thank Vesna Arrigler, Zdenka Držaj, Jolanda Furlan and
568 Mojca Žitko from the Faculty of Chemistry and Chemical Technology, for their technical

569 assistance. We gratefully acknowledge Professor Marjan Veber from the Faculty of
570 Chemistry and Chemical Technology for providing us with access to his laboratory, and
571 Professor Boris Pihlar for his advice on the voltammetric methods. We also thank Dr
572 Christopher P. Berrie for language revision of the manuscript.

573

574 **Appendix. Supplementary Data**

575 Supplementary material associated with this article is provided in the separate document that
576 accompanies the manuscript.

577

578

579 **References**

- 580 Agency for Toxic Substances and Disease Registry (ATSDR), 2004. Toxicological profile for
581 cobalt. U.S. Department of Health and Human Services, Public Health Service,
582 Washington, D.C., USA.
583 <http://www.atsdr.cdc.gov/toxprofiles/tp33.pdf>
- 584 Armbruster, D.A., Pry, T., 2008. Limit of blank, limit of detection and limit of quantitation.
585 *Clin. Biochem. Rev.*, 29, Suppl. 1: S49-S52.
- 586 Baldi, G., Bonacchi, D., Innocenti, C., Lorenzi, G., Sangregorio, C., 2007 Cobalt ferrite
587 nanoparticles: The control of the particle size and surface state and their effects on
588 magnetic properties. *J. Magn. Magn. Mater.* 311, 10–16.
- 589 Čampelj, S., Makovec, D., Drogenik, M., 2008. Preparation and properties of water-based
590 magnetic fluids. *J. Phys. Condens. Matter* 20, 204101 (5pp).
- 591 David, C. A., Galceran, J., Rey-Castro, C., Puy, J., Companys, E., Salvador, J., Monné, J.,
592 Wallace, R., Vakourov, A., 2012. Dissolution Kinetics and Solubility of ZnO
593 Nanoparticles Followed by AGNES. *J. Phys. Chem. C*, **116**, 11758–11767.
- 594 El Badawy, A.M., Silva, R.G., Morris, B., Scheckel, K.G., Suidan, M., Tolaymat, T.M., 2011.
595 Surface Charge-Dependent Toxicity of Silver Nanoparticles. *Environ. Sci. Technol.* 45,
596 283–287.
- 597 Furia, T.E., 1972. Stability Constants (log K₁) of Various Metal Chelates. In Chapter 6 -
598 Sequestrants in Foods. *CRC Handbook of Food Additives*, 2nd ed. CRC Press, Boca
599 Raton, Florida, USA.
- 600 Golobič, M., Jemec, A., Drobne, D., Romih, T., Kasemets, K., Kahru, A., 2012. Upon
601 exposure to Cu nanoparticles, the accumulation of copper in the isopod *Porcellio scaber*
602 is due to the dissolved Cu ions inside the digestive tract. *Environ. Sci. Technol.* 46,
603 12112–12119.

604 Gyergyek, S., Drofenik, M., Makovec, D., 2012. Oleic-acid-coated CoFe₂O₄ nanoparticles
605 synthesized by co-precipitation and hydrothermal synthesis. *Mater. Chem. Phys.* 133,
606 515–522.

607 Hahn, A., Fuhlrott, J., Loos, A., Barcikowski, S., 2012. Cytotoxicity and ion release of alloy
608 nanoparticles. *J. Nanopart. Res.* 14, 686.

609 Hajdú, A., Illés, E., Tombácz, E., Borbáth, I., 2009. Surface charging, polyanionic coating and
610 colloid stability of magnetite nanoparticles. *Colloid Surface A*, 347, 104–108.

611 Hong, S.C., Lee, J.H., Lee, J., Kim, H.Y., Park, J.Y., Cho, J., Lee, J., Han, D.-W., 2011.
612 Subtle cytotoxicity and genotoxicity differences in superparamagnetic iron oxide
613 nanoparticles coated with various functional groups. *Int. J. Nanomed.* 6, 3219–3231.

614 Hopkin, S.P., 1990a. Species-Specific Differences in the Net Assimilation of Zinc, Cadmium,
615 Lead, Copper and Iron by the Terrestrial Isopods *Oniscus asellus* and *Porcellio scaber*.
616 *J. Appl. Ecol.*, 27, 460-474.

617 Hopkin, S.P., 1990b. Critical Concentrations, Pathways of Detoxification and Cellular
618 Ecotoxicology of Metals in Terrestrial Arthropods. *Funct. Ecol.*, 4, 321-327.

619 Horev-Azaria, L., Kirkpatrick, C.J., Korenstein, R., Marche, P.N., Maimon, O., Ponti, J.,
620 Romano, R., Rossi, F., Golla-Schindler, U., Sommer, D., Uboldi, C., Unger, R.E.,
621 Villiers, C., 2011. Predictive Toxicology of Cobalt Nanoparticles and Ions:
622 Comparative In Vitro Study of Different Cellular Models Using Methods of Knowledge
623 Discovery from Data. *Toxicol. Sci.* 122, 489–501.

624 Huang, S., Wang, Z., Ma, M., 2002. Measuring the bioavailable/toxic concentration of copper
625 in natural water by using anodic stripping voltammetry and *Vibrio-qinghaiensis*
626 *sp.Nov.-Q67* bioassay. *Chem. Spec. Bioavailab.*, 15, 37–45.

627 Huang, S., Wang, Z., 2003. Application of anodic stripping voltammetry to predict the
628 bioavailable/toxic concentration of Cu in natural water. *Appl. Geochem.*, 18, 1215–
629 1223.

630 Huynh, K.A., Chen, K.L., 2011. Aggregation Kinetics of Citrate and Polyvinylpyrrolidone
631 Coated Silver Nanoparticles in Monovalent and Divalent Electrolyte Solutions. *Environ.*
632 *Sci. Technol.* 45, 5564–5571.

633 Jiang, C., Hsu-Kim, H., 2014. Direct *in situ* measurement of dissolved zinc in the presence of
634 zinc oxide nanoparticles using anodic stripping voltammetry. *Environ. Sci.: Processes*
635 *Impacts*, in press; DOI: 10.1039/C4EM00278D

636 Jorhem, L., 2004. Certified reference materials as a quality tool in food control: much used—
637 often misused—sometimes abused. *Accred. Qual. Assur.*, 9, 305–310.

638 Lawrence, A.L., McAloon, K.M., Mason, R.P., Mayer, L.M. 1999. Intestinal Solubilization of
639 Particle-Associated Organic and Inorganic Mercury as a Measure of Bioavailability to
640 Benthic Invertebrates. *Environ. Sci. Technol.* 33, 1871–1876.

641 Matzapetakis, M., Dakanali, M., Raptopoulou, C.P., Tangoulis, V., Terzis, A., Moon, N.,
642 Giapintzakis, J., Salifoglou, A., 2000. Synthesis, spectroscopic and structural
643 characterization of the first aqueous cobalt(II)-citrate complex: toward a potentially
644 bioavailable form of cobalt in biologically relevant fluids. *J. Biol. Inorg. Chem.* 5, 469–
645 474.

646 Mayer, L.M., Weston, D.P., Bock, M.J., 2001. Benzo[a]pyrene and zinc solubilization by
647 digestive fluids of benthic invertebrates—a cross-phyletic study. *Environ. Toxicol.*
648 *Chem.* 20, 1890–1900.

649 Meyer, J.S., 2002. The utility of terms “bioavailability” and “bioavailable fraction” for
650 metals. *Mar. Environ. Res.* 53, 417–423.

651 Mirčeski, V., Komorsky-Lovrić, Š., Lovrić, M. *Square-Wave Voltammetry – Theory and*
652 *Application*; Springer-Verlag: Berlin Heidelberg, Germany, 2007.

653 Misra, S. K., Dybowska, A., Berhanu, D., Luoma, S. N., Valsami-Jones, E., 2012. The
654 complexity of nanoparticle dissolution and its importance in nanotoxicological studies.
655 *Sci. Total Environ.*, **438**, 225–232.

656 Mohapatra, S.R., Maiti, S., Maiti, T.K., Panda, A.B., 2011. Monodisperse mesoporous cobalt
657 ferrite nanoparticles: synthesis and application in targeted delivery of antitumor drugs.
658 *J. Mater. Chem.* 21, 9185–9193.

659 Neouze, M.-A., Schubert, U., 2008. Surface Modification and Functionalization of Metal and
660 Metal Oxide Nanoparticles by Organic Ligands. *Monats. Chem.* 139, 183–195.

661 Novak, S., Drobne, D., Golobič, M., Zupanc, J., Romih, T., Gianoncelli, A., Kiskinova, M.,
662 Kaulich, B., Pelicon, P., Vavpetič, P., Jeromel, L., Ogrinc, N., Makovec, D., 2013.
663 Cellular Internalization of Dissolved Cobalt Ions from Ingested CoFe₂O₄ Nanoparticles:
664 In Vivo Experimental Evidence. *Environ. Sci. Technol.* 47, 5400–5408.

665 Nguyen, K.C., Seligy, V.L., Massarsky, A., Moon, T.W., Rippstein, P., Tan, J., Tayabali,
666 A.F., 2013. Comparison of toxicity of uncoated and coated silver nanoparticles. *J. Phys.*
667 *Conf. Ser.* 429, 012025.

668 Papis, E., Rossi, F., Raspanti, M., Dalle-Donne, I., Colombo, G., Milzani, A., Bernardini, G.,
669 Gornati, R., 2009. Engineered cobalt oxide nanoparticles readily enter cells. *Toxicol.*
670 *Lett.* 189, 253–259.

671 Pesavento, M., Alberti, G., Biesuz, R., 2009. Analytical methods for determination of free
672 metal ion concentration, labile species fraction and metal complexation capacity of
673 environmental waters: A review. *Anal. Chim. Acta*, 631, 129–141.

674 Phillips, K.M., Wolf, W.R., Patterson, K.Y., Sharpless, K.E., Holden, J. M., 2007. Reference
675 materials to evaluate measurement systems for the nutrient composition of foods: results

676 from USDA's National Food and Nutrient Analysis Program (NFNAP). *Anal. Bioanal.*
677 *Chem.*, 389, 219–229.

678 Pihlar, B., Valenta, P., Nürnberg, H.W., 1981. New high-performance analytical procedure
679 for the voltammetric determination of nickel in routine analysis of waters, biological
680 materials and food. *Fresen. J. Anal. Chem.*, 307, 337–346.

681 R Core Team. R: A language and environment for statistical computing. R Foundation for
682 Statistical Computing, Vienna, Austria, 2013;
683 <http://www.r-project.org>

684 Ranke, J. ChemCal: Calibration functions for analytical chemistry. R package version 0.1-29,
685 2013;
686 <http://cran.r-project.org/web/packages/chemCal/index.html>

687 Riding, M.J., Doick, K.J., Martin, F.L., Jones, K.C., Semple, K.T., 2013. Chemical measures
688 of bioavailability/bioaccessibility of PAHs in soil: Fundamentals to application. *J.*
689 *Hazard. Mater.* 261, 687–700.

690 Sabbioni, E., Fortaner, S., Farina, M., Del Torchio, R., Petrarca, C., Bernardini, G., Mariani-
691 Costantini, R., Perconti, S., Di Giampaolo, L., Gornati, R., Di Gioacchino, M., 2012.
692 Interaction with culture medium components, cellular uptake and intracellular
693 distribution of cobalt nanoparticles, microparticles and ions in Balb/3T3 mouse
694 fibroblasts. *Nanotoxicology* 8, 88–99.

695 Sigma Aldrich, 2011 (November 22). *Iron(III) nitrate nonahydrate*; MSDS No. 254223
696 [Online]. Retrieved from <http://www.sigmaaldrich.com/catalog/product/aldrich/254223>
697 (accessed May 27, 2013).

698 Sigma Aldrich, 2013 (May 17). *Iron(III) chloride*; MSDS No. 157740 [Online]. Retrieved
699 from <http://www.sigmaaldrich.com/catalog/product/sial/157740> (accessed May 27,
700 2013).

701 Simonsen, L.O., Harbak, H., Bennekou, P., 2012. Cobalt metabolism and toxicology—A brief
702 update. *Sci. Total Environ.* 432, 210–215.

703 Soler, M.A.G., Lima, E.C.D., da Silva, S.W., Melo, T.F.O., Pimenta, A.C.M., Sinnecker, J.P.,
704 Azevedo, R.B., Garg, V.K., Oliveira, A.C., Novak, M.A., Morais, P.C., 2007. Aging
705 Investigation of Cobalt Ferrite Nanoparticles in Low pH Magnetic Fluid. *Langmuir* 23,
706 9611–9617.

707 Tejamaya, M., Römer, I., Merrifield, R.C., Lead, J.R., 2012. Stability of Citrate, PVP, and
708 PEG Coated Silver Nanoparticles in Ecotoxicology Media. *Environ. Sci. Technol.* 46,
709 7011–7017.

710 Tubbing, D.M.J., Admiraal, W., Cleven, R.F.M.J., Iqbal, M., Vandemeent, D., Verweij, W.,
711 1994. The contribution of complexed copper to the metabolic inhibition of algae and
712 bacteria in synthetic media and river water. *Water Res.*, 28, 37–44.

713 Weston, D.P., Maruya, K.A., 2002. Predicting bioavailability and bioaccumulation with in
714 vitro digestive fluid extraction. *Environ. Sci. Technol.* 21, 962–971.

715 World Health Organization (WHO), 2006. Cobalt and inorganic cobalt compounds. Concise
716 international chemical assessment document. WHO Press, World Health Organization,
717 Geneva, Switzerland.

718 <http://www.inchem.org/documents/cicads/cicads/cicad69.htm>

719 Xu, M., Li, J., Hanagata, N., Su, H., Chen, H., Fujita, D., 2013. Challenge to assess the toxic
720 contribution of metal cation released from nanomaterials for nanotoxicology—the case of
721 ZnO nanoparticles. *Nanoscale*, 5, 4763–4769.

722 Zi, Z., Sun, Y., Zhu, X., Yang, Z., Dai, J., Song, W., 2009. Synthesis and magnetic properties
723 of CoFe₂O₄ ferrite nanoparticles. *J. Magn. Magn. Mater.* 321, 1251–1255.

724 Zidar, P., Drobne, D., Štrus, J., 1998. Determination of moult stages of *Porcellio scaber* for
725 routine use. *Crustaceana* 71, 646–654.

726 Zimmer, M., 1997. Surfactants in the gut fluids of *Porcellio scaber* (Isopoda: Oniscoidea),
727 and their interaction with phenolics. *J. Insect Physiol.* 43, 1009–1014.

728 Zimmer, M., Topp, W., 1997. Homeostatic Responses in the Gut of *Porcellio scaber*
729 (Isopoda: Oniscidea) Optimize Litter Degradation. *J. Comp. Physiol. B* 167, 582–585.

730 Zimmer, M., Brune, A., 2005. Physiological Properties of the Gut Lumen of Terrestrial
731 Isopods (Isopoda: Oniscidea): Adaptive to Digesting Lignocellulose? *J. Comp. Physiol.*
732 *B* 175, 275–283.

733

734

735